Photocatalytic degradation of bisphenol A in the presence of TiO$_2$ nanoparticles: Effect of solvent on size control

Fowziya Shaik Ali[a, b], Kezhen Qi[c], Bushra Al Wahaibi[a], Mohammed A. Meetani[d], Haider Al Lawati[a], Younghun Kim[e], Salma M.Z. Al Kindy[a], Rengaraj Selvaraj[a,*]

[a]*Department of Chemistry, College of Science, Sultan Qaboos University, Muscat, Oman, email: srengaraj1971@yahoo.com*
[b]*Department of Chemistry, Khadir Mohideen College, Adirampattinum, Tamil Nadu, India*
[c]*Institute of Catalysis for Energy and Environment, College of Chemistry and Chemical Engineering, Shenyang Normal University, Shenyang, 110034, China*
[d]*Department of Chemistry, College of Science, United Arab Emirates University, Al Ain, UAE*
[e]*Department of Chemical Engineering, Kwangwoon University, Seoul 139-701, Korea*

ABSTRACT

The anatase TiO$_2$ (a-TiO$_2$) nanoparticles with controlled size have been successfully prepared by a facile solution phase method without using any surfactants, employing titanium isopropoxide as precursors in various alcohol (methanol, ethanol, propanol and butanol) media. Both XRD and Raman results revealed that the products are the phase of anatase TiO$_2$. Morphological studies performed by TEM showed that the products were nanoparticles with the particle size in the range of 5–20 nm, the size of a-TiO$_2$ nanoparticles could be easily turned by changing the types of alcohol. The photocatalytic activity studies of the a-TiO$_2$ nanoparticles demonstrated their excellent performance in photodegrading methylene blue and bisphenol aqueous solution by using UV-A light irradiation. This higher photocatalytic activity of the a-TiO$_2$ nanoparticles was mainly attributed to the smaller particle size.

Keywords: Photocatalyst; Solution phase; Bisphenol A; Degradation; TiO$_2$; Optical properties

1. Introduction

The environmental pollution of endocrine disrupting chemicals (EDCs) in water sources has received scientific and public attention over the past decade because EDCs are capable of interfering with normal hormone function through mimicking endogenous hormones [1]. Bisphenol-A [2,2-bis (4-hydroxyphenyl) propane, BPA] is one a kind of endocrine disruption substances. This compound is found in polycarbonate plastics and epoxy resins. Polycarbonate plastics are often used in containers that store food and beverages, such as water bottles, baby bottles and cups. They may also be used in toys and other consumer goods. Epoxy resins can be used to coat the inside of metal products, such as food cans, baby formula cans, bottle tops and

water supply lines [2–3]. The widespread use of BPA and its incomplete removal from wastewaters led to its residual occurrence in urban wastewaters, industrial wastewater, treated effluents, and even drinking waters [4]. Toxicity tests revealed that it may cause various adverse effects on aquatic organisms even at low exposure levels [5]. Due to its various adverse endocrine disrupting effects on aquatic organisms even at low exposure levels, the methods for its effective removal from water is needed impatiently. Several methods have been investigated to remove BPA from aqueous solutions, including biological, ultrasonic, Fenton oxidation, H$_2$O$_2$ oxidation and photocatalytic methods [6–9]. Among these, heterogeneous photocatalytic technology is known as a promising one because of its potential of mineralizing most of the organic pollutants through the generation of highly active reactive oxygen species such as photo-generated hole (h+) and hydroxyl radical (⁻OH) by using UV/Visible light irradiation and semiconductor

*Corresponding author.

materials [10]. Rengaraj and Li found that the photocatalysis process has been successfully used for BPA degradation under UV light irradiation [11].

Titanium dioxide (TiO_2) has been intensively investigated as a model photocatalyst due to its high photocatalytic activity, low cost, high chemical stability and non-toxic nature [12]. However, its real-life application has been restricted by its low utilization of solar energy because of its big band gap (~3.2 eV) and the high recombination rate of photogenerated charge carriers [13]. In the past decades, many efforts have been devoted to enhance the activity of TiO_2-based photocatalysts, such as control of phase [14] and morphology [15,16], nanosize of semiconductor [17], deposition of noble metal [18,19], doping of metal or non-metal atoms [20,21], photo sensitization [22,23], and coupling with a narrow band gap semiconductor [24,25]. Among these methods, nanosized TiO_2 crystals have attracted much attention due to its size-dependent properties. Up to now, many synthesis methods have been developed to synthesize TiO_2 nanocrystals with control size and morphology for enhancing their photocatalytic activity [26]. For instances, Xu et al. [27] successfully prepared the size-controlled anatase TiO_2 nanoparticles by using the hydrothermal method, photocatalystic activity for degradation of methylene blue is increased as the particle size become smaller, especially when the size is less than 30 nm. Kočí et al. [28] successfully synthesized anatase TiO_2 nanoparticles with the diameter in the range of 4.5–29 nm via the sol-gel method, and found that it showed an excellent photocatalytic performance on CO_2 reduction. In these synthesis methods, some long-chain surfactants usually need be used to control the crystal morphology. However, there is a common problem, that is, it is difficult to remove these surfactants and often need to calcine the samples at high temperatures [29]. Thus, it is still of importance to develop a simple method for the synthesis of morphology-controlled TiO_2 crystals without using any surfactants.

In this work, a simple solution phase method has been presented to synthesize morphology-controlled a-TiO_2 nanocrystals without using any organic surfactants. It is found that the size variations of the a-TiO_2 nanoparticles were achieved by simply tuning the length of carbon chain of alcohol. Namely, the size of a-TiO_2 nanoparticles is decreased by increasing the alcohol length of the reaction solution. The photocatalytic activity of prepared a-TiO_2 nanoparticles was also evaluated by using photodegradation of methylene blue (MB) and BPA solution and the result revealed that the smaller size had a higher photocatalytic activity.

2. Experimental section

2.1. Preparation and characterization of a-TiO_2 nanocrystals

Titanium is opropoxide ([$Ti(OC_3H_7)_4$], 99%), methanol (MeOH, 99%), ethanol (EtOH, 99%), propanol (PrOH, 99%), butanol (BuOH, 99%) and toluene (99%) were purchased from Sigma-Aldrich and were employed as received without additional purification. In a typical synthesis, 5 mL of titanium is opropoxide were dissolved in 50 mL of each of the above mentioned solvent, respectively, and continuously stirred for 7 d to form crystals by the hydrolysis at room temperature in a 250 mL beaker. After 7 d the white powder obtained was dried at 80°C in an oven and then calcined at 400°C for 3 h in a nitrogen atmosphere for further characterization.

The crystalline properties of TiO_2 nanocrystals were studied by X-ray diffraction (XRD) using a Bruker (D5005) X-ray diffractometer equipped with graphite monochromatized CuKα radiation (λ = 1.54056 Å). Raman spectroscopy measurements were performed to confirm the structure of the as-prepared products. The Raman spectrometer (Bruker SENTERA 200 LX model) employs a solid-state laser with an excitation wavelength of 532 nm. The crystal morphology was examined by transmission electron microscopy (TEM) (JEOL JEM-3010). The absorption spectra of the as-prepared samples were recorded using a UV-Vis diffuse reflectance spectroscopy (DRS) (Jasco V670) in the wavelength range of 200–1000 nm, with $BaSO_4$ as a reference.

2.2. Photocatalytic activity studies

All photoreaction experiments were carried out in a photocatalytic reactor system, which consists of a cylindrical borosilicate glass reactor vessel with an effective volume of 250 mL, a cooling water jacket, and a UV-A lamp (8 W medium-pressure mercury lamp (Institute of Electric Light Source, Beijing) positioned axially at the center as a visible light. The reaction temperature was kept at 25°C by circulating the cooling water. A special glass frit as an air diffuser was fixed at the reactor to uniformly disperse air into the solution. Photocatalytic activities of the prepared samples were examined by the degradation of MB (Sigma Aldrich 96%) and bisphenol A solution under UV-A light irradiation. For each run the reaction suspension was freshly prepared by adding 0.100 g of catalyst into 250 mL of aqueous MB solution, with an initial concentration of 5 mg L^{-1} and BPA solution with an initial concentration of 10 mg L^{-1}. The aqueous suspension containing pollutant and catalyst was then irradiated under UV-A light with constant aeration. At the given time intervals, the sample was withdrawn from the suspension and centrifuged at 4000 rpm for 15 min to remove the catalyst. The filtrate was analyzed for the degree of the MB and BPA degradation.

2.3. Analytical methods

The absorption spectra were recorded using an UV-vis spectrophotometer (UC-2450-SHIMADZU). The maximum characteristic absorption wavelength of MB was positioned at 597 nm. BPA concentration was analyzed by LC/MS (Agilent Technologies – 6460 Triple quad LC/MS), in which polarity C18 column (Polarity C18, 3 μm, 2.1 × 100 mm, P. No. 186001295) was employed and a mobile phase of acetonitrile/water (64:34), v/v) was used at a flow rate of 0.3 mL/min. An injection volume of 5 μl was used and the amount of BPA was determined by a 6460 Triple quad LC/MS detector.

3. Results and discussion

3.1. Structure and composition determination

XRD measurement was used to investigate the crystal structure the TiO_2 nanoparticles prepared in alcohols with

different carbon length. As shown in Fig. 1, all the XRD patterns of the as-prepared samples can be indexed to the anatase TiO_2 (JCPDS No. 21-1272). The peaks at 25.5°, 37.9°, 48.2°, 53.8°, 55.0°, 63.0°, 69.2°, 70.9° and 75.4°, which represent the indices of (101), (004), (200), (105), (211),(204), (116), (220) and (215) planes of anatase phase appeared [30]. This similar XRD patterns were observed for all samples, indicating that changing carbon length of alcohols does not change the phase of a-TiO_2. The average crystallite sizes of the as synthesized a-TiO_2 samples were calculated using the Scherrer equation from the broadening of the a-TiO_2 (101) facet diffraction peak. The crystallite size of the samples is 22 nm, 19 nm, 14 nm, 13 nm and 7 nm for a-TiO_2-MeOH, a-TiO_2-EtOH, a-TiO_2-PrOH, a-TiO_2-BuOH and a-TiO_2-Toluene, respectively.

The Raman spectroscopy is further employed to examine the crystalline structure of the as-prepared TiO_2 samples, as shown in Fig. 2. The Raman spectrum exhibits two Brillouin zones (BZs) located at 396, 517 and 636 cm^{-1}, which can be identified as B_{1g}, A_{1g} and E_g, respectively. This results agree well with the Raman peaks of bulk anatase TiO_2 [31]. By comparing the Raman spectra, it is clear that the intensities of Raman peaks of a-TiO_2-Toluene shows a dramatically decrease due to the small particle size [32]. Both the Raman and XRD results demonstrate that the as-prepared samples are anatase TiO_2 phase using the different reaction solvent.

3.2. Morphology of samples

Morphologies of the a-TiO_2 nanocrystals prepared in different alcohols are examined by TEM, as shown in Fig. 3. When MeOH was used as the reaction solvent, the diameters of the as-obtained a-TiO_2 nanoparticles were in the range of 20–25 nm. When EtOH was used as the reaction solvent, the diameters were dispersed from 16 to 18 nm. When PrOH was used as the reaction solvent, the diameter was in the range of 12–14 nm. When BuOH was used as reaction solvent, the product was comprised of the smallest nanospheres, about 8–10 nm. When toluene was used as the reaction solvent, the product was comprised of the

nanoparticles with the diameter of 5–8 nm. The crystallite size from the TEM result is consistent with that calculated from the XRD analyses by Scherrer formula. These results indicate that the size of a-TiO_2 nanoparticles could be easily turned by changing the types of alcohol. This phenomenon can be understood as the following reasons:

1. The polarity of the alcohol increases with decreasing the length of the carbon chain, thus the shorter carbon length of alcohol can form stronger bonds with TiO_2 surface than that of longer length. According to Boltzmann distribution, the stronger adsorption will provide a higher density of alcohol molecules on TiO_2 crystal surrounding. The adsorbed alcohol molecules will slow down the rate of growth units moving to the as-growing alcohol crystal surface, which causes the decrease of the nucleation rate of TiO_2 resulting in the formation of bigger particles.
2. Dielectric constant is another important factor to affect the crystal size. The present work demonstrated that the solvent with a higher dielectric constant resulted in bigger a-TiO_2 nanocrystals. Solvents with higher dielectric constants tend to induce slower precipitation kinetics. However, The use of solvents with lower dielectric constant leads to super saturation of the Ti^{2+} ion due to the lower solubility of the titanium salts. This provides the driving force for the nucleation and growth of TiO_2 nanoparticles, i.e., a shortened nucleation time and higher solid particle growth. Also, the dielectric constant of the medium can affect the interparticle forces and hence the growth and size of the resulting particles.

3.3. Optical property

In order to investigate the optical property of the as-prepared a-TiO_2 nanoparticles, the UV-vis adsorption
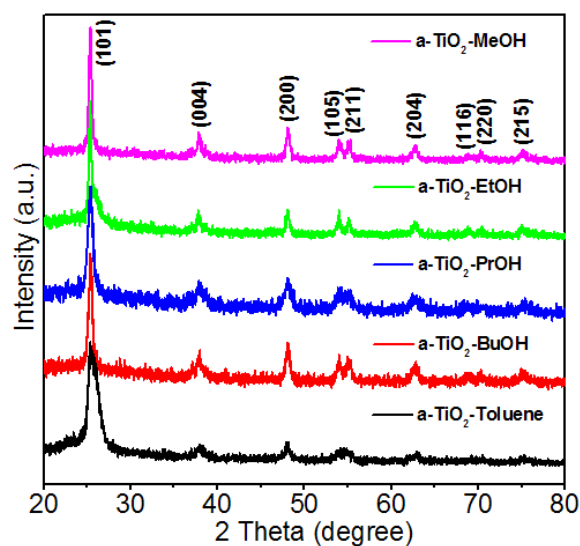

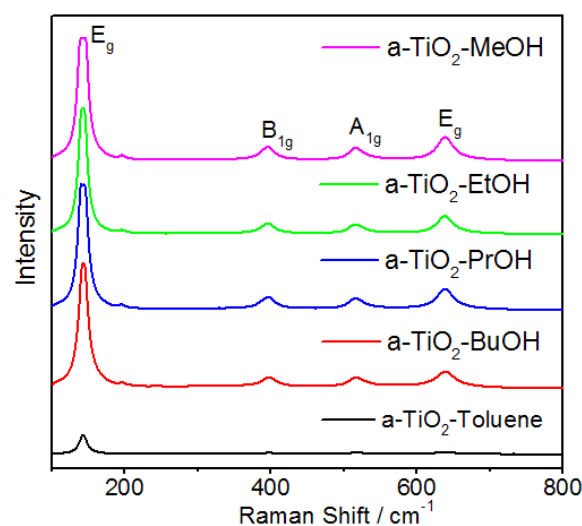Fig. 1. XRD patterns of the samples prepared from various solvents.

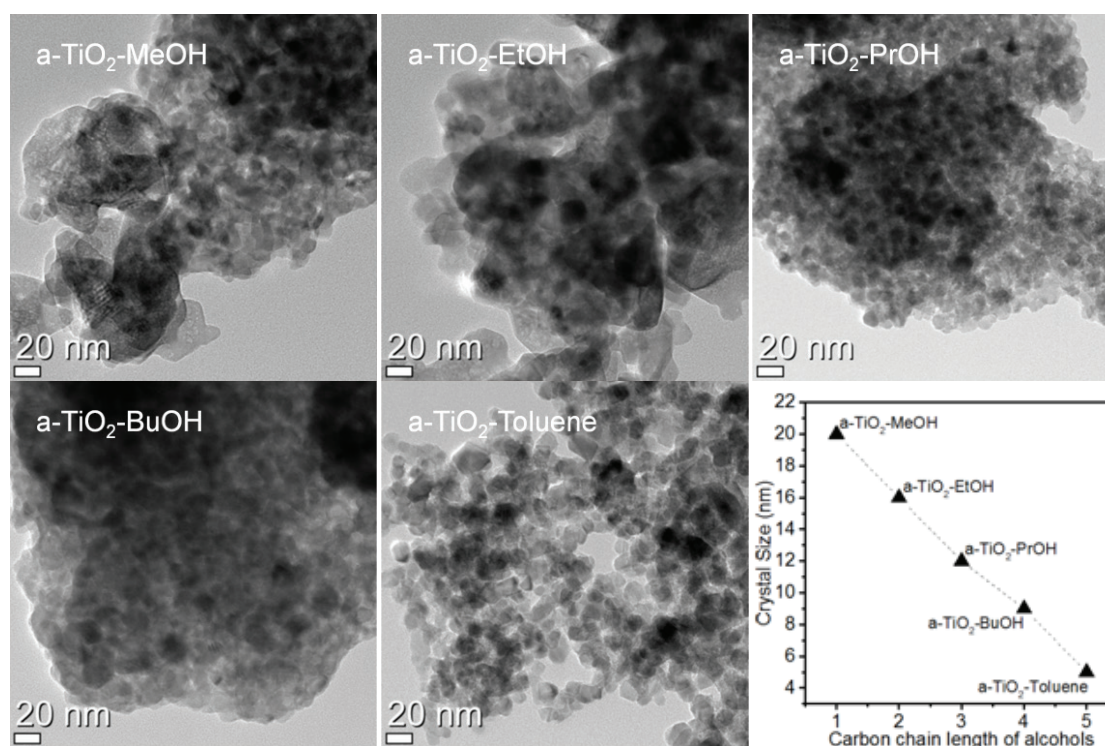Fig. 2. Raman spectra of the samples prepared from various solvents.

Fig. 3. TEM image of the a-TiO$_2$ nanocrystals prepared from various solvents.

Table 1
Crystal size obtain form different alcohol solvent

Sample	Particle size (TEM) (nm)	Crystal size (XRD) (nm)	Dielectric constant	Band gap (eV)
TiO$_2$-MeOH	20	22	32.6	3.05
TiO$_2$-EtOH	16	19	24.3	2.90
TiO$_2$-PrOH	12	14	20.1	2.85
TiO$_2$-BuOH	9	13	17.8	2.82
TiO$_2$-Toluene	5	7	2.4	3.00

spectrum has been measured. Fig. 4 illustrates the DRS spectra of samples a-TiO$_2$-MeOH, a-TiO$_2$-EtOH, a-TiO$_2$-PrOH, a-TiO$_2$-BuOH, a-TiO$_2$-Toluene. The absorption edges of the a-TiO$_2$ nanoparticles are in the range of 400–420 nm. The absorption edge for the samples from a-TiO$_2$-MeOH to a-TiO$_2$-BuOH showed a red shift. The band gap values increased slightly from 2.82 to 3.05 eV as the particle size increased. But the band gap of the a-TiO$_2$-Toluene shows an increase (3.00 eV), which can be attributed to the quantization size effect of the TiO$_2$ nanoparticles [33]. It is expected that this good optical property of the a-TiO$_2$ nanoparticles may offer an opportunity to enhance the photocatalytic activity.

3.4. Photocatalytic performance

The photocatalytic activities of a-TiO$_2$ samples prepared in different solvents were evaluated for the photocatalytic degradation of MB dye under UV-A light irradiation. Fig. 5
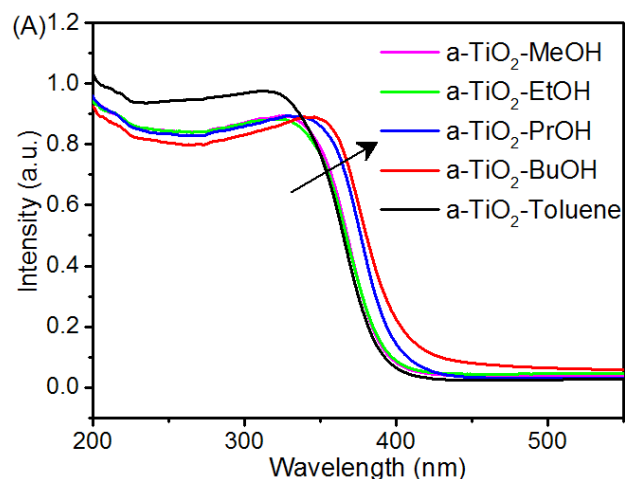

Fig. 4. UV-vis DRS spectra for the a-TiO$_2$ samples prepared in different solvents.

shows the photocatalytic activity for the degradation of MB under UV-A light irradiation over all the a-TiO$_2$ samples. After addition of catalyst into the MB solution, the photocatalytic activity of a-TiO$_2$ nanocrystals can be well tuned as a function of the crystal size, as shown in Fig. 6. With a decrease of the size of the crystal from 22 to 7 nm, TiO$_2$ nanocrystals exhibited greatly enhanced photocatalytic performance, the order of the photocatalytic activity is a-TiO$_2$-Toluene > a-TiO$_2$-BuOH > a-TiO$_2$-PrOH > a-TiO$_2$-EtOH > a-TiO$_2$-MeOH. That is because that the smaller size can provide more active position.
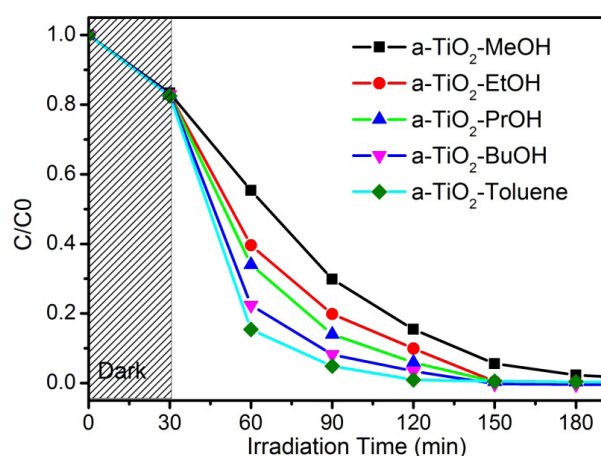
Fig. 5. Photocatalytic performance of the prepared photocatalysts for degrading MB for the a-TiO$_2$ nanocrystals as prepared from various alcohols.
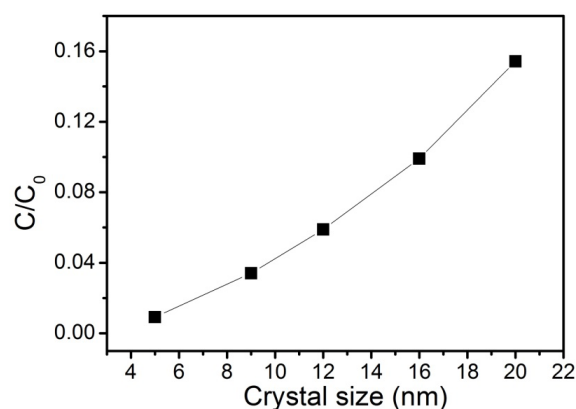

Fig. 7. Photocatalytic degradation of BPA (10 mg/L, 250 mL) by TiO$_2$ nanoparticles (100 mg) under UV light irradiation.

Fig. 6. Photocatalytic performance for degradation of MB related to the size of a-TiO$_2$ nanocrystals as prepared from various alcohols.

Fig. 8. The time-dependent LC/MS peak intensity of the BPA solution (10 mg/L, 250 mL) in the presence of TiO$_2$ nanoparticle under UV-A light.

In order to determine the photocatalytic activity of TiO$_2$ nanoparticles on the degradation of BPA can only be performed after having reached the adsorption equilibrium, since, otherwise, the initial rate of disappearance of a pollutant would simultaneously include both the initial rate of adsorption and the true, initial photocatalytic rate of reaction. The standard solution of BPA used had an initial concentration of 10 mg/l and the volume used as 250 ml. The amount of BPA adsorbed on the TiO$_2$ samples were measured at the end of predetermined time in the dark and the corresponding absorbance spectrum were noted. From that LC/MS peak intensity (Fig. 7) we can clearly understand that there was no much difference in the initial and after adsorbed concentration. This could be evidence for the removal of BPA purely by photocatalytic degradation not by adsorption.

In order to evaluate the photocatalytic activity of TiO$_2$ (from Toluene), a set of experiments for BPA degradation with an initial concentration of 10 mg L^{-1} under UV-A light irradiation was carried out in aqueous suspension using TiO$_2$, and the experimental results are shown in
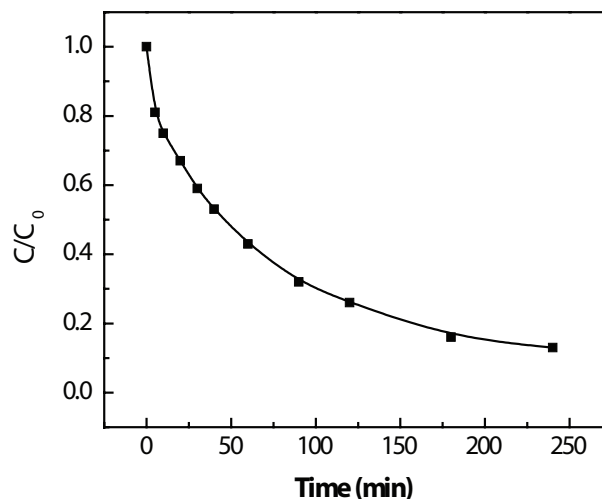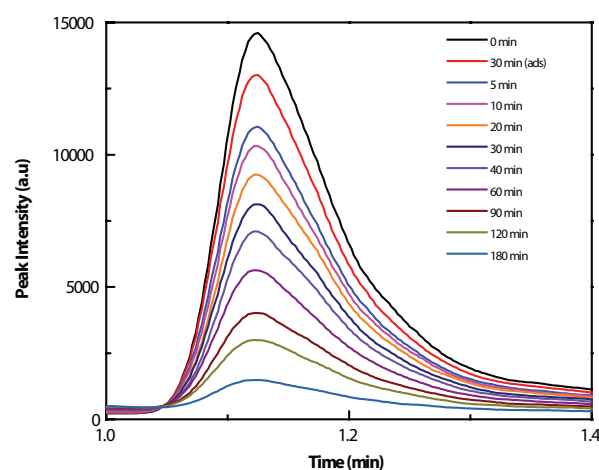
Fig. 7. Fig. 8 represents the time-dependent LC/MS peak intensity of the BPA solution during photo degradation in the presence of TiO$_2$ nanoparticles. The peak intensity at around 1.1 min decreased gradually with irradiation time. At the end of the degradation after 240 min, no peak could be detected, implying that complete oxidation of BPA occurred due to the presence of TiO$_2$ nanoparticle under UV-A light irradiation. The experimental results demonstrated that after 180 min reaction, BPA in the suspensions were reduced by more than 80%. The LC/MS degradation profile of BPA is presented in Figs. 7 and 8, where the rapid removal of BPA can be observed. Here, TiO$_2$ surface favors the migration of photogenerated electron to oxygen molecule, thus improving the electron/hole separation. The enhanced reduction of oxygen through better electron–hole separation in pure TiO$_2$ increases the rates of BPA degradation. The presence of two methyl groups in BPA were initially attacked with ·OH and/or ·OOH radicals having

strong oxidizing power, followed by the cleavage of the two phenyl moieties. Finally, the photomineralisation of CO_2 gas occurred via oxidative processes involving carboxylic acids and aldehydes. Fig. 7 displays the time-dependent LC/MS peak intensity of the BPA solution during photo degradation in the presence of TiO_2 (prepared with Toluene) nanoparticles. The peak at around 1.1 min decreased gradually with irradiation time. At the end of the degradation, no peak could be detected, implying that complete oxidation of BPA occurred due to the presence of TiO_2 under UV light irradiation.

4. Conclusion

A simple method was reported to prepare a-TiO_2 nanocrystals by a simple surfactant-free solution phase process. The XRD and Raman analysis confirmed that the products are in anatase TiO_2 phase. TEM analysis revealed the as-prepared a-TiO_2 nanoparticles with a diameter from 5 nm to 20 nm. The a-TiO_2 nanoparticles exhibited excellent performance in photodegradation of MB and BPA aqueous solution under UV-A light illumination. This higher photocatalytic activity of the a-TiO_2 nanoparticles was attributed to the smaller particle size.

Notes

The authors declare no competing financial interest.

Acknowledgements

References

[1] L. Luo, Y. Yang, A. Zhang, M. Wang, Y. Liu, L. Bian, F. Jian, X. Pan, Hydrothermal synthesis of fluorinated anatase TiO_2/reduced graphene oxide nanocomposites and their photocatalytic degradation of bisphenol A, Appl. Surf. Sci., 353 (2015) 469–479.

[2] O. Bechambi, L. Jlaiel, W. Najjar, S. Sayadi, Photocatalytic degradation of bisphenol A in the presence of Ce–ZnO: Evolution of kinetics, toxicity and photodegradation mechanism, Mater. Chem. Phys., 173 (2016) 95–105.

[3] K. Narsaiah, S.N. Jha, R. Bhardwaj, R. Sharma, R. Kumar, Optical biosensors for food quality and safety assurance—a review, J. Food Sci. Technol., 49 (2012) 383–406.

[4] Y. Ding, P. Zhou, H. Tang, Visible-light photocatalytic degradation of bisphenol A on $NaBiO_3$ nanosheets in a wide pH range: A synergistic effect between photocatalytic oxidation and chemical oxidation, Chem. Eng. J., 291 (2016) 149–160.

[5] Y.T. Xie, H.B. Li, L. Wang, Q. Liu, Y. Shi, H.Y. Zheng, M. Zhang, Y.T. Wu, B. Lu, Molecularly imprinted polymer microspheres enhanced biodegradation of bisphenol A by acclimated activated sludge, Water Res., 45 (2011) 1189–1198.

[6] L. Yu, C. Wang, X. Ren, H. Sun, Catalytic oxidative degradation of bisphenol A using an ultrasonic-assisted tourmaline-based system: Influence factors and mechanism study, Chem. Eng. J., 252 (2014) 346–354.

[7] H. Katsumata, S. Kawabe, S. Kaneco, T. Suzuki, K. Ohta, Degradation of bisphenol A in water by the photo-Fenton reaction, J. Photochem. Photobiol. A., 162 (2004) 297–305.

[8] M. Molkenthin, T. Olmez-Hanci, M.R. Jekel, I. Arslan-Alaton, Photo-Fenton-like treatment of BPA: Effect of UV light source and water matrix on toxicity and transformation products, Water Res., 47 (2013) 5052–5064.

[9] J. Xia, J. Di., S. Yin, H. Li, H. Xu, Li Xu, H. Shu, M. He, Solvothermal synthesis and enhanced visible-light photocatalytic decontamination of bisphenol A (BPA) by g-C_3N_4/BiOBr heterojunctions, Mater. Sci. Semicond. Process, 24 (2014) 96–103.

[10] C. Guo, M. Ge, L. Liu, G. Gao, Y. Feng, Y. Wang, Directed synthesis of mesoporous TiO_2 microspheres: catalysts and their photocatalysis for Bisphenol A degradation, Environ. Sci. Technol., 44 (2010) 419–425.

[11] S. Rengaraj, X.Z. Li, Photocatalytic degradation of bisphenol A as an endocrine disruptor in aqueous suspension using Ag-TiO_2 catalysts, Int. J. Environ. Pollut., 27 (2006) 20–37.

[12] A. Fujishima, K. Honda, Electrochemical photolysis of water at a semiconductor electrode, Nature, 238 (1972) 37–38.

[13] L. Pan, J. Zou, X. Zhang, L. Wang, Water-mediated promotion of dye sensitization of TiO_2 under visible light, J. Am. Chem. Soc., 133 (2011) 10000–10002.

[14] D.W. Hu, W.X. Zhang, Y. Tanaka, N. Kusunose, Y. Peng, Q. Feng, Mesocrystalline Nanocomposites of TiO_2 polymorphs: topochemical mesocrystal conversion, characterization, and photocatalytic response, Cryst. Growth Des., 15 (2015) 1214–1225.

[15] Q.L. Xu, J.G. Yu, J. Zhang, J.F. Zhang, G. Liu, Cubic anatase TiO_2 nanocrystals with enhanced photocatalytic CO_2 reduction activity, Chem. Commun., 51 (2015) 7950–7953.

[16] A. Meng, J. Zhang, D. Xu, B. Cheng, J. Yu, Enhanced photocatalytic H_2-production activity of anatase TiO_2 nanosheet by selectively depositing dual-cocatalysts on {101} and {001} facets, Appl. Catalysis–B: Environ., 198 (2016) 286–294.

[17] S.W. Liu, J.Q. Xia, J.G. Yu, Amine-functionalized titanate nanosheet-assembled yolk@shell microspheres for efficient cocatalyst-free visible-light photocatalytic CO_2 reduction, ACS Appl. Mater. Interfaces, 7 (2015) 8166–8175.

[18] N. Lakshminarasimhan, A. Bokare, W. Choi, Effect of agglomerated state in mesoporous TiO_2 on the morphology of photodeposited Pt and photocatalytic activity, J. Phys. Chem. C, 116 (2012) 17531–17539.

[19] L. Qi, W. Ho, J. Wang, P. Zhang, J. Yu, Enhanced catalytic activity of hierarchically macro-/mesoporous Pt/TiO_2 toward room-temperature decomposition of formaldehyde, Catal. Sci. Technol., 5 (2015) 2366–2377.

[20] J. Choi, H. Park, M.R. Hoffmann, Effects of single metal-ion doping on the visible-light photoreactivity of TiO_2, J. Phys. Chem. C, 114 (2010) 783–792.

[21] M.S. Akple, J. Low, Z. Qin, S. Wageh, A.A. Al-Ghamdi, J. Yu, S. Liu, Nitrogen-doped TiO_2 microsheets with enhanced visible light photocatalytic activity for CO_2 reduction, Chinese J. Catal., 36 (2015) 2127–2134.

[22] Z.C. Lian, P.P. Xu, W.C. Wang, D.Q. Zhang, S.N. Xiao, X. Li, G.S. Li, C_{60}-decorated CdS/TiO_2 mesoporous architectures with enhanced photostability and photocatalytic activity for H_2 evolution, ACS Appl. Mater. Interf., 7 (2015) 4533–4540.

[23] K. Qi, R. Selvaraj, T.A. Fahdi, S. Al-Kindy, Y. Kim, G. Wang, C. Tai, M. Sillanpää, Enhanced photocatalytic activity of anatase-TiO_2 nanoparticles by fullerene modification: A theoretical and experimental study, Appl. Surf. Sci., 387 (2016) 750–758.

[24] I. Robel, M. Kuno, P.V. Kamat, Size-dependent electron injection from excited CdSe quantum dots into TiO_2 nanoparticles, J. Am. Chem. Soc., 129 (2007) 4136–4137.

[25] L. Li, B. Cheng, Y. Wang, J. Yu, Enhanced photocatalytic H_2-production activity of bicomponent NiO/TiO_2 composite nanofibers, J. Colloid Interface Sci., 449 (2015) 115–121.

[26] W.J. Ong, L.L. Tan, S.P. Chai, S.T. Yong, A.R. Mohamed, Facet-dependent photocatalytic properties of TiO_2 based composites for energy conversion and environmental remediation, Chem. Sus. Chem., 7 (2014) 690–719.

[27] N.P. Xu, Z.F. Shi, Y.Q. Fan, J.H. Dong, J. Shi, M.Z.-C. Hu, Effects of particle size of TiO$_2$ on photocatalytic degradation of methylene blue in aqueous suspensions, Ind. Eng. Chem. Res., 38 (1999) 373–379.

[28] K. Kočí, L. Obalová, L. Matějová, D. Plachá, Z. Lacný, J. Jirkovský, O. Šolcová, Effect of TiO$_2$ particle size on the photocatalytic reduction of CO$_2$, Appl. Catal. B: Environ., 89 (2009) 494–502.

[29] J.Q. Yan, G.J. Wu, N.J. Guan, L.D. Li, Z.X. Li, X.Z. Cao, Understanding the effect of surface/bulk defects on the photocatalytic activity of TiO$_2$: anataseversus rutile, Phys. Chem. Chem. Phys., 15 (2013) 10978–10988.

[30] T. Sreethawong, Y. Suzuki, S. Yoshikawa, Synthesis, characterization, and photocatalytic activity for hydrogen evolution of nanocrystalline mesoporous titania prepared by surfactant-assisted templating sol–gel process, J. Solid State Chem., 178 (2005) 329–338.

[31] T. Mazza, E. Barborini, P. Piseri, P. Milani, Raman spectroscopy characterization of TiO$_2$ rutile nanocrystals, Phys. Rev. B, 75 (2007) 045416-1-5.

[32] X.X. Xue, W. Ji, Z. Mao, H.J. Mao, Y. Wang, X. Wang, W.D. Ruan, B. Zhao, J.R. Lombardi, Raman investigation of nano-sized TiO$_2$: effect of crystallite size and quantum confinement, J. Phys. Chem. C, 116 (2012) 8792–8797.

[33] L. Bras, Electron–electron and electron-hole interactions in small semiconductor crystallites: The size dependence of the lowest excited electronic state, J. Chem. Phys., 80 (1984) 4403–4409.